

A Framework for Collecting Data:
Revising Sensor Synchronization Methods

by

Sara Gonzalez

Submitted to the Department of Mechanical Engineering
in Partial Fulfillment of the Requirements for the Degree of

Bachelor of Science in Mechanical Engineering

at the

Massachusetts Institute of Technology

June 2017



ARCHIVES

©2017 Massachusetts Institute of Technology. All rights reserved.

Signature redacted

Signature of Author:

Department of Mechanical Engineering

Signature redacted

Certified by:

Leia Stirling
Associate Professor of Aeronautics and Astronautics
Thesis Supervisor

Signature redacted

Certified by:

Rohit Karnik
Associate Professor of Mechanical Engineering
Undergraduate Officer

A Framework for Collecting Data:
Revising Sensor Synchronization Methods

by

Sara Gonzalez

Submitted to the Department of Mechanical Engineering
on May 12, 2017 in Partial Fulfillment of the
Requirements for the Degree of

Bachelor of Science in Mechanical Engineering

ABSTRACT

Data collection is frequently carried out in research, as well as in industry for purposes ranging from quality control to assessing system limits. However, several complications may arise to hinder optimal data collection and analysis, including synchronization of different data types from a variety of sensors. A benchtop model was designed with the primary goal of understanding human-spacesuit interactions through the collection and analysis of force, pressure, and internal kinematics data. This thesis addresses shortcomings in the setup that led to difficulty in data analysis and synchronization and presents a revised framework for collecting these data. A system was designed such that the start of each trial of data collection can be synced across the three types of sensors: a load cell, a pressure mat, and inertial measurement units.

Thesis Supervisor: Leia Stirling

Title: Associate Professor of Aeronautics and Astronautics

Acknowledgments

I would like to express my thanks to Professor Leia Stirling and to Aditi Gupta for their mentorship and guidance over the past few months during which I was a part of their research group. Professor Stirling helped rekindle my love of engineering by being a true role model for women in engineering –intelligent, strong, kind, and understanding. I would like to thank Aditi for familiarizing me with the nature of the project and for providing advice, direction, and support throughout this thesis project. Our weekly meetings were invaluable for this work. I am also grateful to Conor Cullinane and Christopher King who offered me their assistance on various aspects of the project.

I would also like to express my gratitude to Dr. Barbara Hughey whose expertise and assistance was vital for this work. Furthermore, I would like to thank Hosea Siu and Stephen Banzaert for their help on electronics aspects of this work.

Table of Contents

Abstract	2
Acknowledgements	3
Table of Contents	4
List of Figures	5
List of Tables	6
1. Introduction	7
1.1 Background and Previous Work	7
1.1.1 Hardware used in Former Benchtop Model	8
1.1.2 Challenges	10
1.2 Thesis Overview	11
2. Results from Former Benchtop Model	12
3. Design of Benchtop System	17
3.1 Force Setup	17
3.1.1 Load Cell Selection	17
3.1.2 Mechanical Considerations	18
3.1.3 Electronic Considerations	19
3.2 Synchronization	21
4. Experimental Evaluation	24
4.1 Force Data Collection	24
4.2 Testing Synchronization	25
5. Discussion and Conclusion	27
5.1 Conclusion	27
5.2 Future Work	27
6. References	29
7. Appendices	30
Appendix A: Specification Sheets	30
Appendix B: Futek Load Cell Certificate of Conformance	34

List of Figures

Figure 1a: Model leg	9
Figure 1b: Pressure mat geometry for the front of the leg	10
Figure 1c: Pressure mat geometry for the back of the leg	10
Figure 2a: Tensile force vs. normalized time for Zone B trials	12
Figure 2b: Tensile force vs. normalized time for Zone D trials	13
Figure 2c: Tensile force vs. normalized time for Zone C trials	14
Figure 2d: Peak pressures of the front of the leg	15
Figure 2e: Peak pressures of the back of the leg	16
Figure 3a: Load cell mount assembly	19
Figure 3b: Strap assembly prototype	19
Figure 3c: Simplified Analog Devices AD8237 instrumentation amplifier schematic	21
Figure 3d: Synchronization setup schematic	23
Figure 4a: Schematic for evaluation of force data collection	25
Figure 4b: Schematic for evaluation of synchronization	26

List of Tables

Table 3: Pugh chart comparing possible load cells against a set of criteria

18

1. Introduction

1.1 Background and Previous Work

Data are numerical outputs that have been and continue to be used for the quantification of systems. Measuring data is important in both a research setting and in industry. In industry, measurements may be taken to validate a model, verify system requirements, or assess system limits. Measurement of fatigue cycles on cracks, for example, may be used for quality control of artificial heart valves in medical device manufacturing [1]. The measurements taken for the project described by this thesis are used to validate a computational model. However, measuring data sometimes proves to be a challenge due to geometry constraints, sensor availability, and a variety of other obstacles. For instance, choosing an instrument with the improper dynamic range for a particular experiment will cause saturation for signal amplitudes that are too high or will cause the signal to get lost in the noise if the amplitude is too low [2]. Once useful data are collected, they must be analyzed to extract useful parameters in order to convey meaningful results. Synchronization of different types of data may also be necessary to characterize a system because it allows for the examination of one or more data sets in the context of others. Synchronization across different sensors calls for forethought in data collection methods, including choice of sample rate and sensor selection.

Over the last few decades, the Man Vehicle Laboratory has worked to optimize human-vehicle system effectiveness and safety. This thesis focuses on the work of one group in the lab, which is currently examining human-spacesuit interactions, specifically in the upper and lower leg. Knowledge of human-spacesuit interaction can inform on possible injury mechanisms to the human, and which locations on the body are most susceptible to injury from the interaction. This research is being conducted with the ultimate goal of creating a computational model of a human musculoskeletal system that accurately predicts these interactions. No such model currently exists, so all spacesuit manufacturing to date have been endeavors of trial and error. The computational model would create a way to simulate interactions, and thus test the spacesuit before manufacturing it. This saves resources, not limited to time and money, from failed or non-optimal spacesuit models.

Four types of data are considered for the preliminary characterization of interactions of the leg and spacesuit: pressure, force, internal kinematics, and external kinematics. Pressure data serve to quantify the actual interactions between the human and the spacesuit, while the force and kinematics data provide context for the interactions. These data sets inform a basic, but meaningful musculoskeletal system in which muscle-joint interactions can be determined from force and internal kinematics, and human-spacesuit interactions can be visualized by pressure profiles. Force data, internal kinematics data, and pressure data were collected in the former benchtop model using the setup described in Section 1.1.1. Only three data sets were collected with the former model, but moving forward the model will be revised to include the collection of external kinematic data.

1.1.1 Hardware used in Former Benchtop Model

The testing apparatus used in initial testing consisted of a model leg made of an 80/20 aluminum skeleton with a PVC pipe housing, shown in Figure 1a. A 4-inch diameter PVC pipe was used for the upper leg and a 3-inch diameter PVC pipe was used for the lower leg. The model leg was placed in a spacesuit, and then the spacesuit was pressurized to 1 psig. Force, pressure, and internal kinematics data were collected as the leg was flexed and then extended within the pressurized spacesuit.

Internal actuation of the leg was ruled out due to the associated difficulty of powering and wiring a motor within the pressurized spacesuit; instead the leg was actuated externally via a string attached to an Ametek® Chatillon™ DFE Digital Force Gauge, which was pulled at the ankle to flex or extend the leg. The force gauge served the purpose of force data collection, and pulling on the force gauge provided the actuation necessary to move the leg. Force data were collected by video capture of the force gauge, which has a display update rate of 10 Hz. This footage was imported into Logger Pro® and examined at the default frame rate of 29.98 frames per second. Force values in pound-force were recorded manually from the observed force gauge footage on Logger Pro® and plotted on Excel, with unreadable values omitted.

APDM Opal inertial measurement units (IMUs) were used to collect data of the internal kinematics of the leg at a sampling rate of 128 Hz. They were mounted onto the skeleton by 3D printed rings seen in Figure 1a, which in turn were attached to the skeleton by angle brackets.



Figure 1a. Model leg. The skeleton of the leg is composed of 80/20 aluminum stock. A hinge joint acts as a knee and limits the degrees of freedom available to the leg to one. The black rings shown on the skeleton serve to hold IMUs, which are used to collect data about internal kinematics of the leg. The PVC pipes displayed on the right act as the housing and provide the surface where pressure interactions between the suit and the leg occur.

A novel pliance®-x pressure sensor mat, composed of a 16 x 16 matrix of pressure sensors, was placed on the surface of the PVC pipes to collect data on pressure distribution at four regions of the leg, referred to as zones. This data was collected at a rate of 50 Hz using the pliance®-x system. Three trials were conducted for each zone, where one trial consists of flexing the leg and then extending it. The four zones are defined below, and their geometries are displayed in Figures 1b and 1c.

- Zone A –back of the upper leg
- Zone B –front of the upper leg
- Zone C –front of the lower leg
- Zone D –back of the lower leg

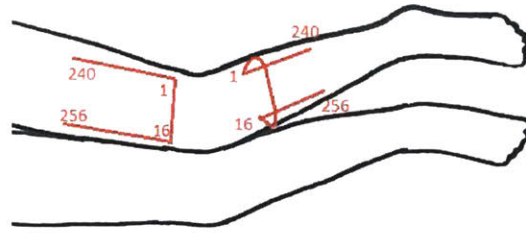


Figure 1b. Pressure mat geometry for the front of the leg. The numbers in red refer to the sensor number of 16 x 16 sensor pressure mat. Sensors 1-16 are located closest to the knee and subsequent rows of sensors are located further away, ending with sensors 240-256. These sensor numbers inform on the location of pressures on pressure maps, like those of peak pressure presented in Figure 2d. Zone B is the region on the front of the upper leg and Zone C is the region on the front of the lower leg.

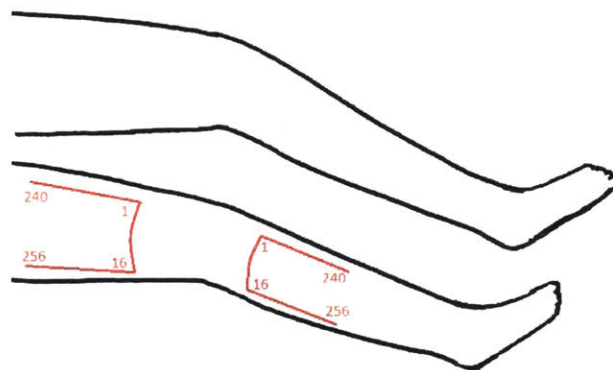


Figure 1c. Pressure mat geometry for the back of the leg. The numbers in red refer to the sensor number of 16 x 16 sensor pressure mat. Sensors 1-16 are located closest to the knee and subsequent rows of sensors are located further away, ending with sensors 240-256. These sensor numbers inform on the location of pressures on pressure maps, like those of peak pressure presented in Figure 2e. Zone A is the region on the back of the upper leg and Zone D is the region on the back of the lower leg.

1.1.2 Challenges

Shortcomings in the aforementioned test setup led to difficulty in attaining force data and in synchronizing data from the three types of sensors. Force data was recorded manually using Logger Pro software to look at videos taken of the force gauge at the default 29.98 fps, which proved to be a tedious process. These force values were later used to create plots of force vs. time and force vs. normalized time, which give some insight into the actuation of the leg. Torque

data calculated from force values give a better understanding of actuation though characterizing torque vs. internal joint angle profiles, when paired with internal kinematics data from the IMUs. However, the IMU data has been difficult to analyze so that extracting these joint angles from the data is an ongoing process.

Synchronization also proved to be a problem because there was no reliable method in place for visualizing the beginning of each trial, as the IMUs would start collecting and storing data as soon as they are undocked. In addition, data taken with the IMUs and pressure mat were taken at different sampling rates, 128 Hz and 50 Hz, respectively.

1.2 Thesis Overview

This thesis focuses on overcoming the challenges described in Section 1.1.2 by designing a revised framework for collecting data. The remainder of this thesis details the approach to constructing the sensor synchronization plan.

Chapter 2 provides results from the former framework used to collect data. It informs the various design choices of the revised benchtop testing system described in Chapter 3. Chapter 4 gives the results of some tests that were performed to evaluate the functionality of the system. Chapter 5 wraps up with a discussion of the results and suggestions for future work and areas for improvement.

2. Results from Former Benchtop Model

Force data were collected by video capture of an Ametek® Chatillon™ DFE Digital Force Gauge, which has a display update rate of 10 Hz. This footage was imported into Logger Pro® and examined at the default frame rate of 29.98 frames per second. Force values in pound-force were recorded manually from the observed force gauge footage on Logger Pro® and plotted on Excel, with unreadable values omitted. Force data for Zone B and Zone D trials, presented in Figure 2a and Figure 2b, respectively, show that the force profiles are similar for the two zones. Additionally, there is consistency across each flexion trial of these zones, as well as across each extension trial, as expected.

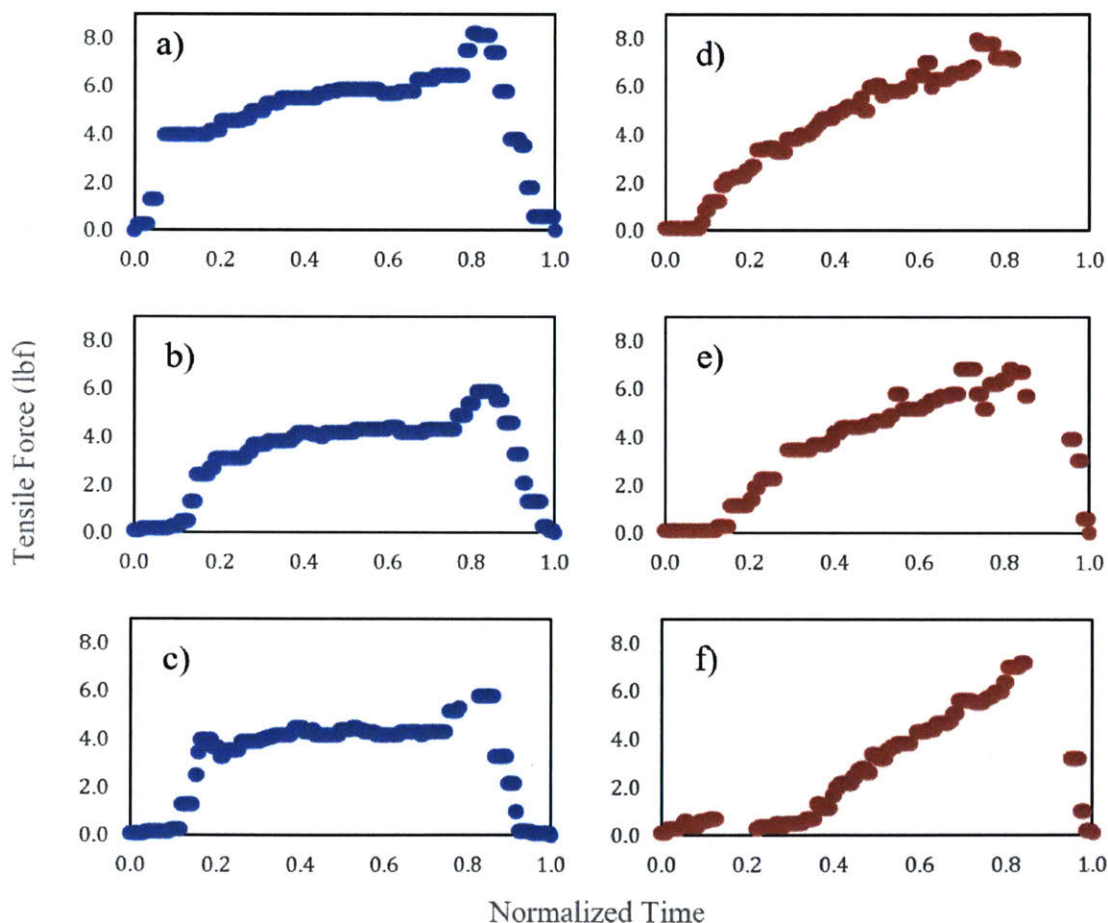


Figure 2a. Tensile force vs. normalized time for Zone B trials. The plots on the left are the force profiles for flexion of the leg for a) trial 1 b) trial 2 and c) trial 3. The plots on the right are the force profiles for extension of the leg for d) trial 1 e) trial 2 and f) trial 3.

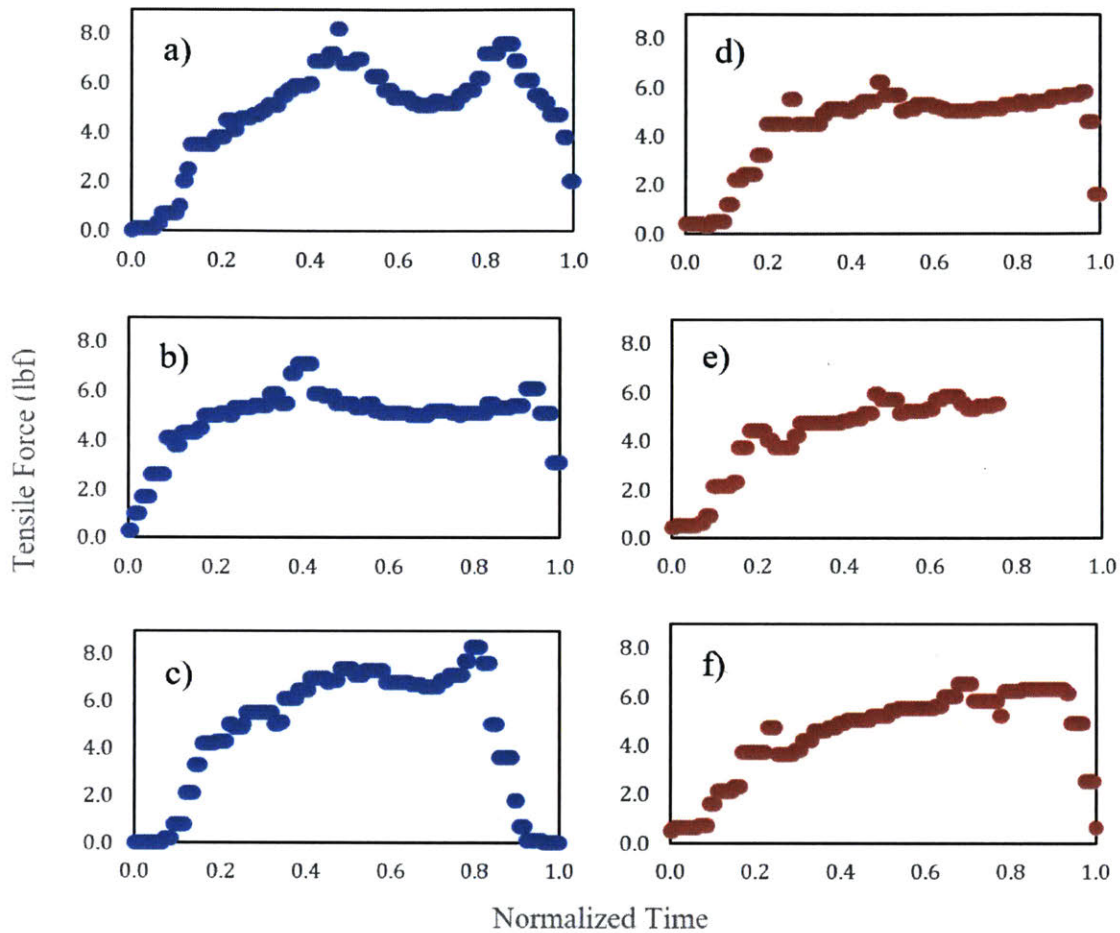


Figure 2b. Tensile force vs. normalized time for Zone D trials. The plots on the left are the force profiles for flexion of the leg for a) trial 1 b) trial 2 and c) trial 3. The plots on the right are the force profiles for extension of the leg for d) trial 1 e) trial 2 and f) trial 3.

Force data for Zone C are displayed in Figure 2c. They present a similar profile with regard to shape to those of Zones B and D in Figures 2a and 2b, but with a different range of values, as evidenced by the bounds of the y-axes. This may be because the 4-inch diameter PVC pipe, representing the upper leg, moved out of place when running trials for this zone.

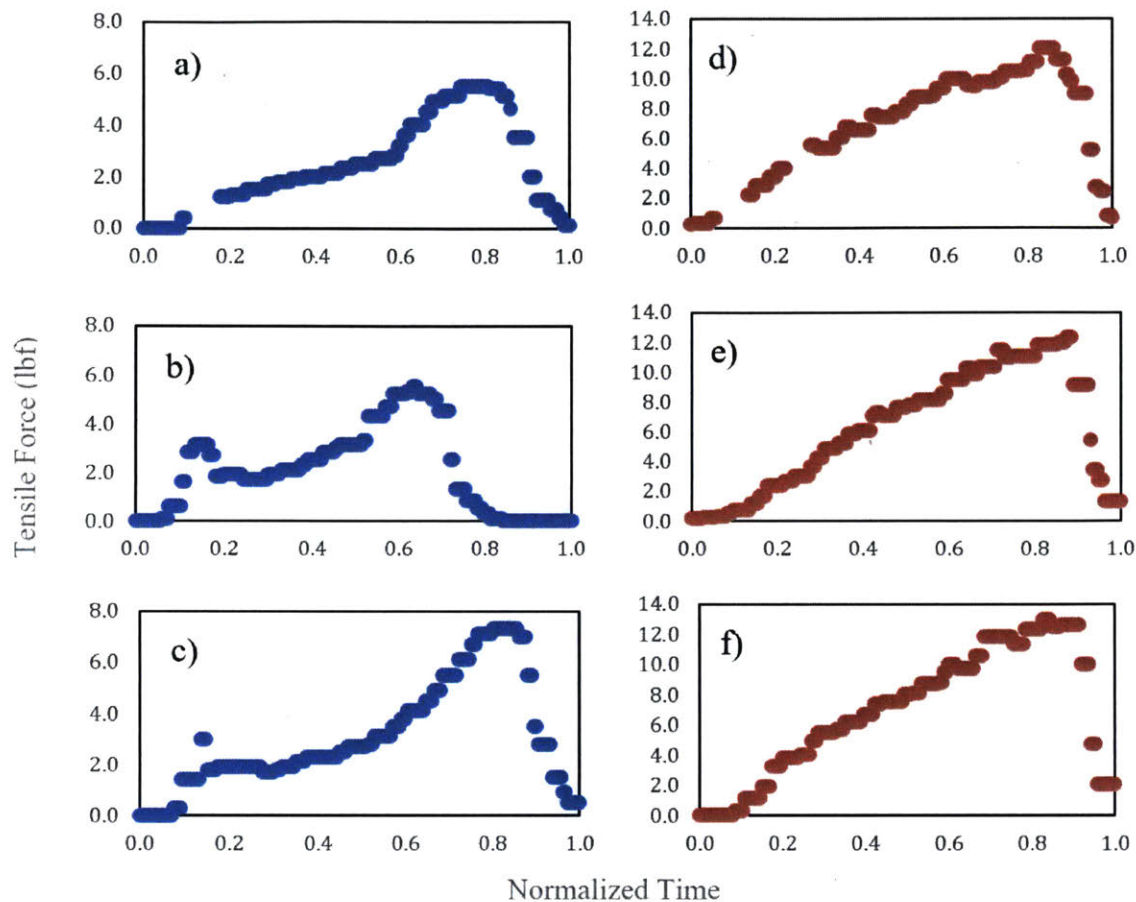


Figure 2c. Tensile force vs. normalized time for Zone C trials. The plots on the left are the force profiles for flexion of the leg for **a)** trial 1 **b)** trial 2 and **c)** trial 3. The plots on the right are the force profiles for extension of the leg for **d)** trial 1 **e)** trial 2 and **f)** trial 3.

Force data for Zone A trials are not presented in this work because there were several issues while running the trials for this zone, as the procedure was not yet finalized. Torque data in pound-feet were calculated from the force values for each trial of Zones B, C, and D given a distance from the axis of rotation of 9.5 inches using the torque formula $\tau = r F \sin\theta$. Torque data is necessary to examine torque as a function of internal joint angle of the leg. The extraction of joint angles from the IMU data is, however, still in progress.

Pressure profiles from the sensor mat were analyzed. Peak pressures at each location of the mat are shown in Figure 2d and Figure 2e, where Figure 2d shows the peak pressure profile for the front of the leg, given the geometry localization of Figure 1b, and Figure 2e shows the

peak pressure profile for the back of the leg, given the geometry localization of Figure 1c. These peak pressure data are significant because they determine safety of a human being; if the pressures are too high, they may cause injury. The pressure profile of Zone D over the three trials provided insight into the location of interaction pressures. During flexion of the leg, the interaction pressures occurred near the knee in each of the three trials. Interaction pressures were found in this same location during extension in Trials 2 and 3.

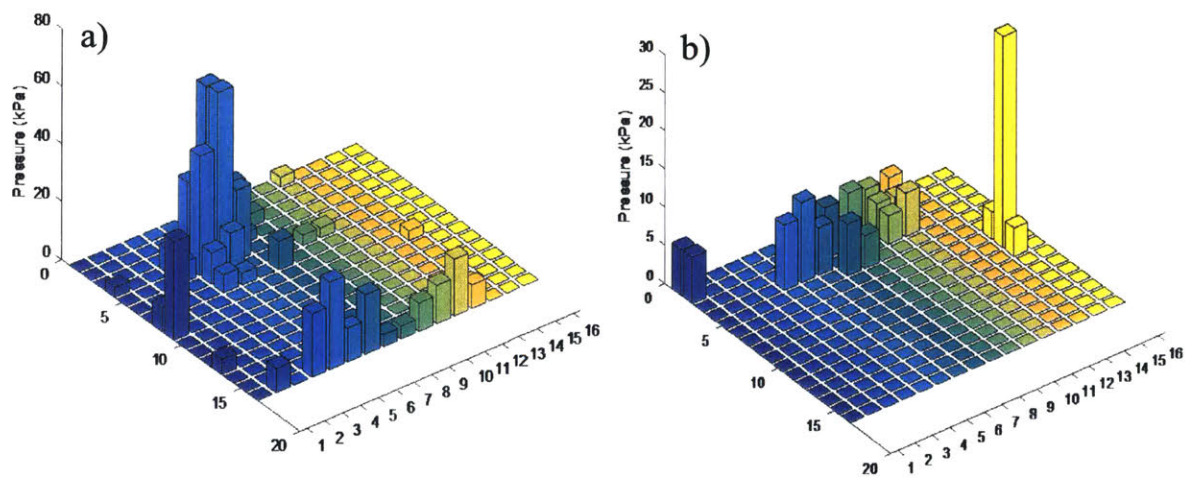


Figure 2d. Peak pressures of the front of the leg. **a)** Zone B profile **b)** Zone C profile. The geometry of the pressure mat on the front of the leg is shown in Figure 1b. Sensors 1-16 are located closest to the knee and subsequent rows of sensors are located further away, ending with sensors 240-256. Note the different axes bounds for the two graphs.

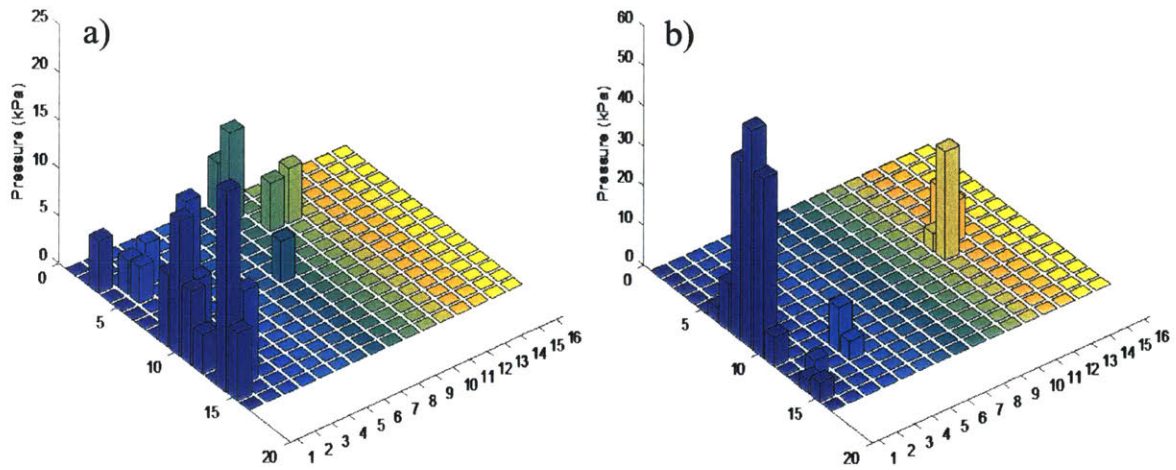


Figure 2e. Peak pressures of the back of the leg. **a)** Zone A profile **b)** Zone D profile. The geometry of the pressure mat on the front of the leg is shown in Figure 1c. Sensors 1-16 are located closest to the knee and subsequent rows of sensors are located further away, ending with sensors 240-256. Note the different axes bounds for the two graphs.

3. Design of Benchtop System

The benchtop system for future data collection was designed with the challenges expressed in Section 1.1.2 in mind, particularly those related to force data collection and synchronization, as well as the results obtained from the former model described in Chapter 1.

3.1 Force Setup

3.1.1 Load Cell Selection

The first design decision for the force setup of the benchtop system was to computerize the collection of data to a greater extent than that of the former system, described in Section 1.1.1. A load cell was selected as the type of sensor to replace the Ametek® Chatillon™ DFE Digital Force Gauge. Various factors were considered when selecting the specific load cell. The videos of the previous force data collection showed that there was a high probability of some off-center loading during experimentation. This excluded S-Beam load cells, which are sensitive to extraneous load, torque, and moments. Additionally off-center loading has been determined to reduce the service life of S-Beam load cells [3]. The two types of load cells considered after this point, considering the need for measuring tension and the likely dynamic range of 0 lbf to 15 lbf, were low profile load cells and single point load cells. Research into several different brands of load cells led to the selection of two brands within budget whose performance specifications were exceptional: Omega and Futek.

A low profile cell from Omega, the LC201 Subminiature Load Cell, and a single point cell from Futek, the LSM300 Load Cell, were selected as the final two candidates for the force setup. The Omega LC201 subminiature load cell was considered due to its use in a different part of the research and, therefore, its availability and financial advantage. Ultimately, the Futek LSM300 load cell was selected because of its greater robustness, excellent performance specifications, and ease of mounting, as seen in Table 3.

Table 3. Pugh chart comparing possible load cells against a set of criteria. The Omega LC201 load cell was used as a reference. Accuracy includes linearity, hysteresis, and repeatability.

Selection Criteria	Load Cells Considered					
	Interface 1500	Omega LCHD	Omega LC201	Futek LSM300	Futek LCF300	Tecsis XLUN294
Accuracy	+	+	0	+	0	+
Cost	-	-	0	0	-	-
Ease of integration	0	0	0	+	0	0
Availability	-	-	0	-	-	-
Size	-	+	0	+	-	-
+	1	2	0	3	0	1
0	1	1	5	1	0	1
-	3	2	0	1	3	3
Net Score	-2	0	0	2	-3	-1

Once the Model LSM300 load cell was selected, the capacity of the load cell was finalized. The force data from testing with the former model gave a maximum force value of approximately 14 lbf seen in Figure 2c. Since resolution scales with capacity, the lowest capacity load cell with this number in its range was selected; thus a 25 lb capacity load cell was chosen over a 10 lb and 50 lb capacity load cell.

3.1.2 Mechanical Considerations

The selection of the single point load cell allowed for a simple mount design. The load cell assembly shown in Figure 3a consists of the load cell, a mount with a built-in handle for pulling, and a spacer to keep the load cell's active beam area from contacting any surface. The three components are held together by two #6 bolts and nuts. The load cell assembly also consists of a strap that goes around the ankle to flex or extend the leg. The previous strap was a piece of string with one end tied around the ankle and the other end tied to the force gauge. The string was noted to have a significant amount of slack in the force gauge videos, and so a strap, which minimized the amount of string, was designed. This strap, presented by the prototype in

Figure 3b makes use of Velcro and metal rings in addition to string. The string is then tied to a rod end that is affixed to the load cell via a threaded rod adapter.



Figure 3a. Load cell mount assembly. The mount and spacer of the physical assembly were designed on SolidWorks and exported to be 3D printed from ABS in a LulzBot TAZ 6 printer.

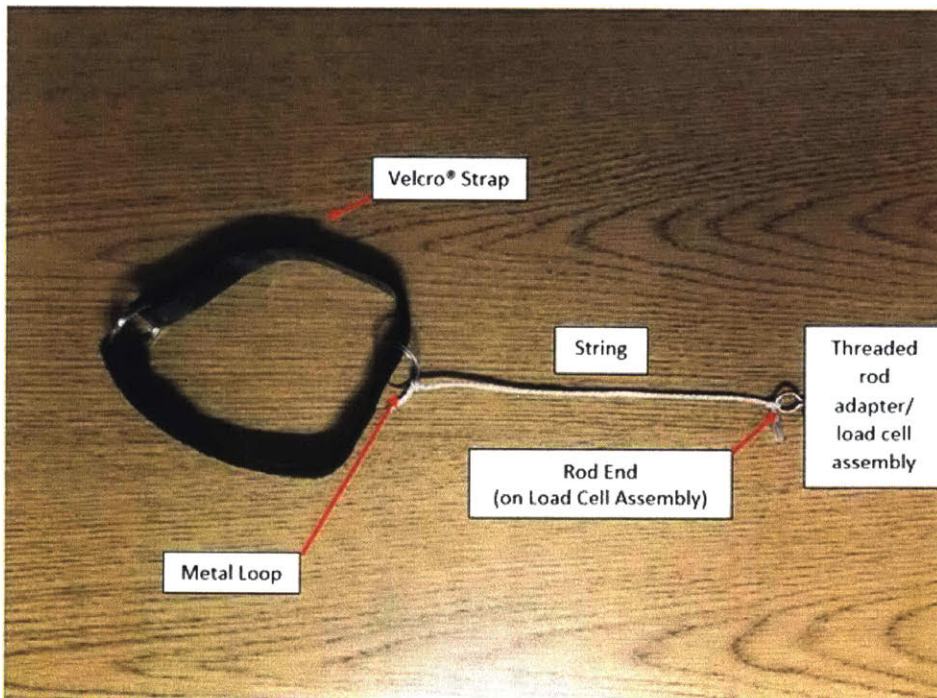


Figure 3b. Strap assembly prototype. The prototype was made out of materials on hand and tested by pulling on a cylindrical object to validate its performance in actuating the leg.

3.1.3 Electronic Considerations

The electronic specifications of the selected Futek LSM300 load cell constrained the setup of the force data collection, as well as its geometry discussed in Section 3.1.2. The load cell has a 4-conductor cable, where two of the wires are used to provide the excitation voltage and the other two are used to send out the signal. An Arduino™ UNO was selected to collect the signal from the load cell via one of the analog pins since the Arduino™ can provide the signal necessary for synchronization, described in Section 2.2.

The maximum excitation given on the specification sheet for the load cell is 18 V (Appendix A); however, a 10 V excitation was recommended by a Futek representative when Product Inquiry was contacted. Following the recommendation of the representative, a 10 V excitation was favored for the load cell over the 18 V maximum. Since an Arduino™ was selected to play a role in force data collection and synchronization, the idea of using the Arduino™ to power the load cell was considered; however, an Arduino™ can only provide a 5 V output. A 10 V excitation voltage was chosen over a 5 V excitation voltage because it would yield a better resolution. Since the Arduino™ can only supply 5 V, two options were considered to provide the 10 V excitation voltage to the load cell: create a circuit to amplify the Arduino™ output or use a power supply. While the circuit could possibly keep the wiring more compact and organized, the power supply was selected because it could more reliably output 10 V.

With the selected 10 V excitation voltage and a nominal rated output of 2 mV/V (Appendix A), the load cell would produce a signal between 0 mV and 20 mV for loads within its capacity of 25 lbs. This voltage difference is too small to be picked up by an Arduino™ so an instrumentation amplifier, Analog Devices AD8237, was selected to interface between the load cell and Arduino™. The 10 V power supply and instrumentation amplifier are shown in the schematic in Figure 3d. The instrumentation amplifier allows for the user to set the desired gain by choosing two external resistors, positioned as shown in Figure 3c. The gain is determined by the resistors by Equation 1, as follows:

$$G = 1 + \frac{R2}{R1} \quad (1)$$

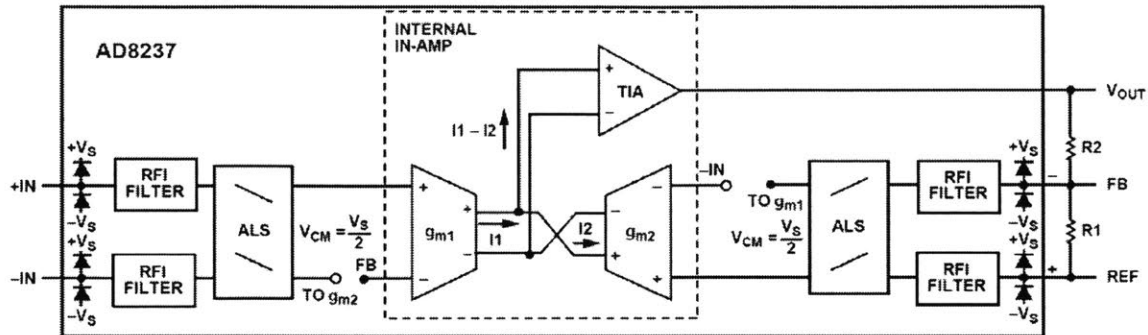


Figure 3c. Simplified Analog Devices AD8237 instrumentation amplifier schematic (Appendix A). The external resistors, R1 and R2, which set the gain are on the right side.

Resistance values $R1 = 1 \text{ k}\Omega$ and $R2 = 390 \text{ k}\Omega$ were selected from standard resistor values to give a gain of 391 by Equation 1. This value of gain was chosen because it would yield a signal of approximately 4.4 V from the maximum force seen in Figure 2c of about 14 lbf, which is safely within the ground to 5 V range that can be accurately measured by the analog input pins of the Arduino™ [4]. The measured voltages are then collected and recorded in MATLAB as forces using the load cell calibration factor of 1.16 lbf/mV that was obtained by Futek during a calibration test and presented on the load cell's Certificate of Conformance (Appendix B).

3.2 Synchronization

Along with the Arduino™ UNO, a pliance®-x Wired Sync Box and an APDM Sync Box were used for synchronization of force, pressure, and kinematics data. The system designed for synchronization across the force, pressure, and kinematics data is shown in Figure 3d. The evaluation of this system is detailed in Section 4.2.

Both the pliance®-x Wired Sync Box and the APDM Sync Box can either send or receive a signal so that the start of a trial can be synced. The pliance®-x Wired Sync Box is connected to the novel pliance®-x box, which transmits data to the computer [5]. The APDM Sync Box is connected to the Access Point, which is the wireless communication hub between the host computer and Opal IMUs. The use of an Arduino™ for collecting the load cell signal led

to the decision to use a trigger input for the external sync boxes rather than a trigger output because of the Arduino's ability to output 5 V. A constant trigger was selected over an edge trigger in the sync setup tab of the novel pliance® online software, so that pressure data collection occurs as long as the signal is 5 V. Similarly, a level trigger type was selected in the external synchronization tab of the Motion Studio software, so that kinematics data collection occurs as long as the input signal is 5V.

A MATLAB script was developed to begin data collection for each trial. Through the use of a Graphical User Interface (GUI) on MATLAB, the user can press a “Start” button to start collecting data and a “Stop” button to stop collecting data. When the “Start” button is pressed, the Arduino™ sends out 5 V to both the pliance®-x Wired Sync Box and the APDM Sync Box from one of its digital output pins and begins reading load cell data through one of its analog input pins. The Arduino™ continues collecting data from the load cell through the instrumentation amplifier and outputting a 5 V signal to the sync boxes until the user presses the “Stop” button on the GUI. The load cell data are converted into force values using the calibration factor of 1.16 lbf/mV and the selected gain of 391 and logged in MATLAB, saved as a .csv file.

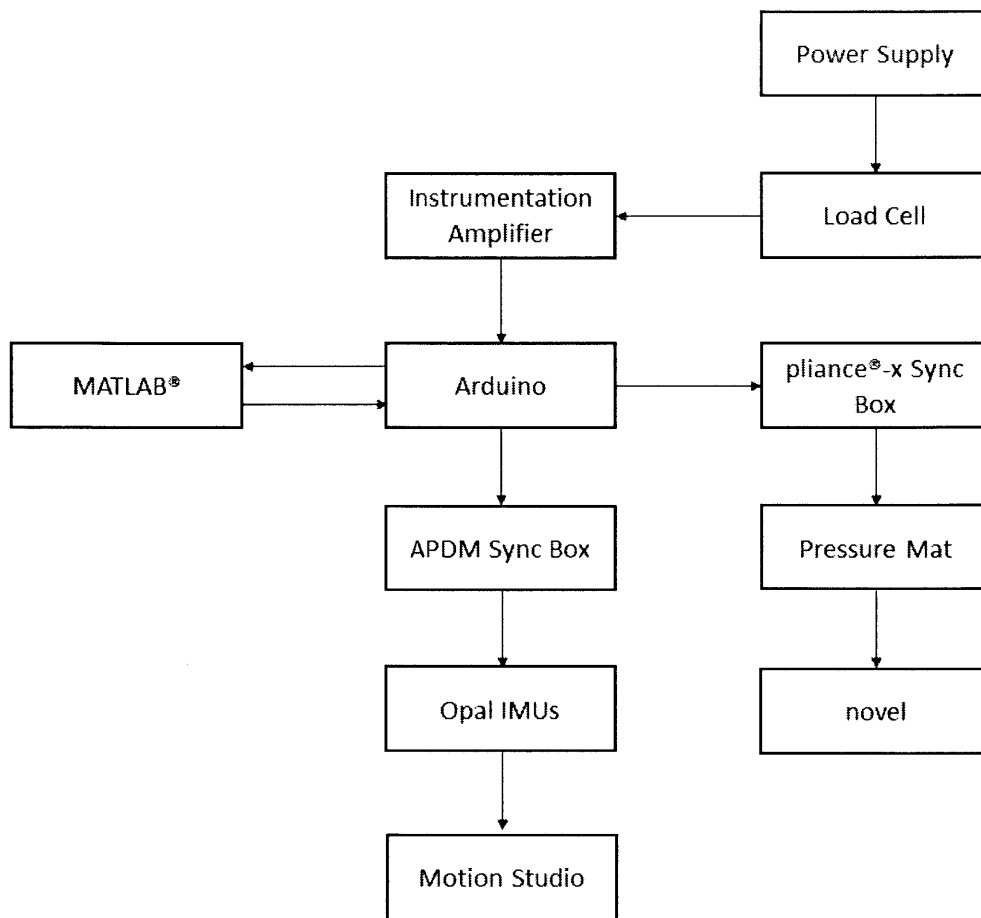


Figure 3d. Synchronization setup schematic. The power supply provides a 10 V excitation voltage to the load cell, which then has its signal amplified by the instrumentation amplifier. When the “Start” button is pressed on the GUI in MATLAB, the voltage is and measured by an Arduino™ analog pin. The data are transmitted to MATLAB and converted to force recorded using the calibration factor of 1.16 lbf/mV and gain factor of 391. Pressure and kinematics data collection are synced with the force data collection through the same GUI. The MATLAB code has the Arduino™ output 5 V to the two sync boxes once the “Start” button is pressed on the GUI, prompting the novel system to collect pressure data from the sensor mat and the APDM system to collect kinematics data from the IMUs. Data collection is terminated for force, pressure, and kinematics when the “Stop” button is pressed.

4. Experimental Evaluation

4.1 Force Data Collection

The force data collection was validated using a different instrumentation amplifier than the selected Analog Devices AD8237, which is expected to arrive in the next few weeks. A readily available Vernier Instrumentation Amplifier was used to amplify the signal from the selected load cell. The nature of the Vernier instrumentation amplifier called for the need of a Vernier Arduino™ Interface shield, as shown in Figure 4a. The interface shield did not allow for the coincident evaluation of force data collection and synchronization because it monopolized the inputs and outputs of the Arduino, such that the Arduino™ could not output the 5 V signal necessary to trigger the two external sync boxes.

The MATLAB code for force data collection was validated, as data was successfully collected and recorded on MATLAB for the modified code accounting for the specifications of the Vernier Instrumentation Amplifier. The Vernier instrumentation amplifier as a set of fixed gains, unlike the Analog Devices AD 8237 instrumentation amplifier which allows the user to set the gain by the selection of two external resistors, as described in Section 3.1.3. A gain of 150 was used for the 0-20 mV range of the Vernier instrumentation amplifier. With the known calibration factor of the load cell, the code only reflected the discrepancy between the gain factors of the different instrumentation amplifiers.

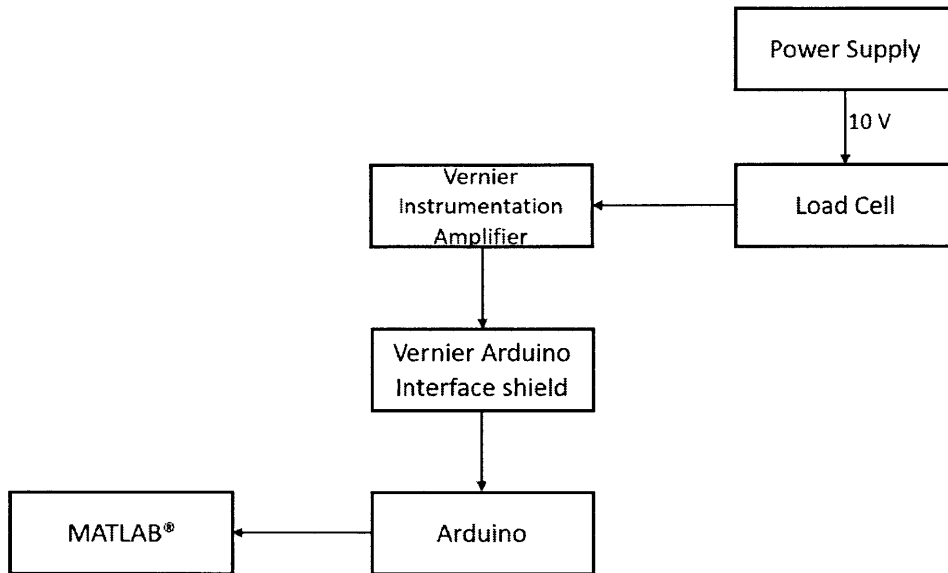


Figure 4a. Schematic for evaluation of force data collection. The power supply provides a 10 V excitation voltage to the load cell, which then has its signal amplified by the Vernier Instrumentation Amplifier. The amplified signal from the Vernier sensor is connected to the Arduino™ microcontroller via the Vernier Arduino™ Interface Shield. The data are transmitted to MATLAB and converted to force recorded using the calibration factor of 25 lbf/20 mV and the known gain factor of 150 for the 0-20 mV range of the Vernier instrumentation amplifier.

4.2 Testing Synchronization

Without a proper instrumentation amplifier for the purposes of the designed synchronization system shown in Figure 3d, synchronization of data collection was tested without a load cell. Instead, voltage readings between 0 V and 5 V from a power supply were measured by the Arduino™ without amplification. The voltage read by the Arduino™ was converted into pseudo force data with a calibration factor in MATLAB. In this way, the power supply acted as the load cell with amplified signal. Syncing the beginning of data collection using the “Start” button on the MATLAB GUI was evaluated with the system shown in Figure 4b. When the “Start” button was pressed, the Arduino™ would send out a 5 V signal to the pliance®-x sync box to trigger data collection for the pressure sensor pad and to the APDM sync

box to trigger data collection for the IMUs at the same time as it started collecting voltage data from the power supply to log in MATLAB. The 5 V output from the Arduino™ at the selection of the “Start” button on the GUI was confirmed by a multimeter. Additionally, the novel and Motion Studio software showed that data collection began when the Arduino™ output to the sync boxes changed from 0 V to 5 V. The “Stop” button was similarly tested; this testing confirmed that both software programs stopped data collection when the Arduino™ output changed from 5 V to 0 V at the press of the button.

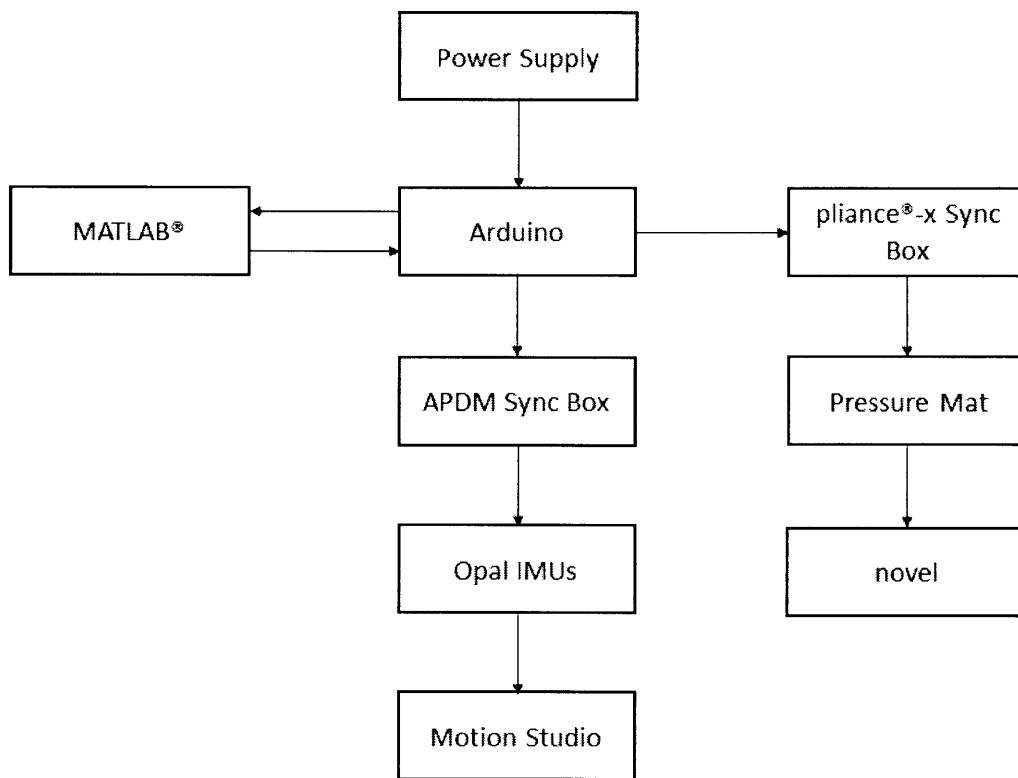


Figure 4b. Schematic for evaluation of synchronization. The power supply outputting a signal between 0 V and 5V replaces the load cell and instrumentation amplifier in testing for force data collection. When the “Start” button is pressed on the GUI in MATLAB, the voltage from the power supply is and measured by an Arduino™ analog pin. The data are transmitted to MATLAB and converted to pseudo force data using the calibration factor of 3 lbf/V. Pressure and kinematics data collection are synced with the force data collection through the same GUI. The MATLAB code has the Arduino™ output 5 V to the two sync boxes once the “Start” button is pressed on the GUI, prompting the novel system to collect pressure data from the sensor mat and the APDM system to collect kinematics data from the IMUs. Data collection is terminated for force, pressure, and kinematics when the “Stop” button is pressed.

5. Conclusion

5.1 Conclusion

The challenges and results of testing with the former benchtop model described in Chapters 1 and 2 informed the design decisions used to revise the methods used for data collection and sensor synchronization. Overall, the evaluation of the revised framework proved it to be better than the former one. The separate evaluation of force data collection and synchronization demonstrates that the GUI and code developed for synchronization across the force, pressure, and kinematics data trials is working correctly. Force data is successfully logged in MATLAB, which overcomes the challenge of force data collection through video footage of a force gauge display described in Sections 1.1.1 and 1.1.2. The implication is that synchronization of data collection can be achieved at the start of each trial, which can be used for model validation and thus enable evaluation of human-suit interactions in terms of force and internal kinematics.

5.2 Future Work

Future work for the proposed system involves testing force data collection and synchronization with the selected instrumentation amplifier once it arrives. Collection of external kinematics data can also be integrated into a future model using the same synchronization design proposed in the thesis with the incorporation of additional IMUs.

Other work that would improve the proposed synchronization system for the purposes of preliminary characterization of interactions of the leg and spacesuit include decreasing the profile of the entire setup. The current system, with the use of the pliance®-x Wired Sync Box, requires the entire system to be placed inside the pressurized spacesuit due to wiring constraints. Although the synchronization of the designed system has been validated, it would be meaningless in this setting since the load cell would be inside the spacesuit, rather than outside and access to the “Start” and “Stop” buttons on the GUI would be obstructed. Using a pliance®-x Wireless Sync Unit instead of the Wired one in the future would enable use of the system within a pressurized spacesuit.

Once the synchronization across the three types of sensors is validated and the system can be used in the pressurized spacesuit, the results of force, pressure, internal kinematics, and external kinematics data throughout the trials can be used to characterize the interactions, pursuing the ultimate goal of creating a musculoskeletal model.

6. References

- [1] Marrey, R. V., Burgermeister, R., Grishaber, R. B., and Ritchie, R. O., 2006, "Fatigue and Life Prediction for Cobalt-Chromium Stents: A Fracture Mechanics Analysis," *Biomaterials*, **27**, pp. 1988-2000.
- [2] Huber, D. M., and Runsten, R. E., 2014, *Modern Recording Techniques*, Focal Press, New York, NY, pp. 492-504.
- [3] *Load Cell Field Guide*, 2015, Interface, Scottsdale, AZ, pp. 11-16.
- [4] "Arduino/Genuino UNO," Arduino™ - ArduinoBoardUno. [Online]. Available: <https://www.arduino.cc/en/main/arduinoBoardUno>
- [5] *pliance-x system manual*, 2013, novel, St. Paul, MN, Chap. 5.

7. Appendices

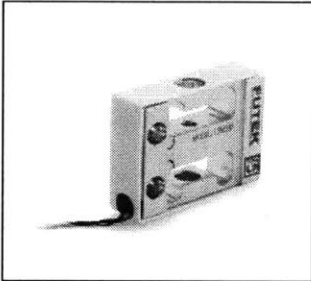
Appendix A: Specification Sheets

A-1: Futek LSM300 Load Cell available online at <http://www.futek.com/product.aspx?t=load&m=lsm300>



FUTEK
ADVANCED SENSOR TECHNOLOGY, INC.

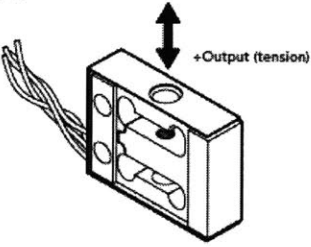
MODEL LSM300
OEM Load Cell



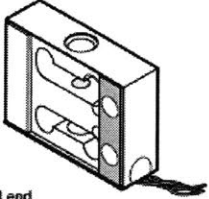
FEATURES

- Intended for high volume applications
- Easily integrates into OEM applications
- Built-in overload protection
- Exceptional nonlinearity and nonrepeatability
- Can integrate with analog VDC, mA, digital SPI, I2C, RS-232, UART output, and more

Active end



Fixed end



SPECIFICATIONS	
PERFORMANCE	
Nonlinearity	±0.02% of RO (2.2-100 lb) ±0.06% of RO (200 lb)
Hysteresis	±0.02% of RO (2.2-100 lb) ±0.06% of RO (200 lb)
Nonrepeatability	±0.02% of RO
Creep	±0.025% of Load
ELECTRICAL	
Rated Output (RO)	2 mV/V nom
Excitation (VDC or VAC)	18 max
Bridge Resistance	1000 Ohm nom
Insulation Resistance	≥500 Mohm @ 50 VDC
Connection	#29 AWG, 4 conductor, spiral teflon cable, 6 in [152.4 mm] long
Wiring/Connector Code	WC2
MECHANICAL	
Weight (approximate)	1 oz [28 g] (2.2-100 lb) 3 oz [85 g] (200 lb)
Safe Overload	See chart on next page
Material	Aluminum (2.2-100 lb), 17-4 PH stainless-steel (200 lb)
IP Rating	IP30
TEMPERATURE	
Operating Temperature	-60 to 200°F [-50 to 93°C]
Compensated Temperature	60 to 160°F [15 to 72°C]
Temperature Shift Zero	±0.005% of RO/°F [0.01% of RO/°C]
Temperature Shift Span	±0.005% of Load/°F [0.01% of Load/°C]
CALIBRATION	
Calibration Test Excitation	10 VDC
Calibration (standard)	Certificate of Conformance
Calibration (available)	5-pt Tension and Compression
Shunt Calibration Value	150 kOhm
CONFORMITY	
RoHS	2011/65/EU
CE	EN61326-1:2006

Sensor Solution Source
Load - Torque - Pressure - Multi-Axis - Calibration - Instruments - Software

www.futek.com





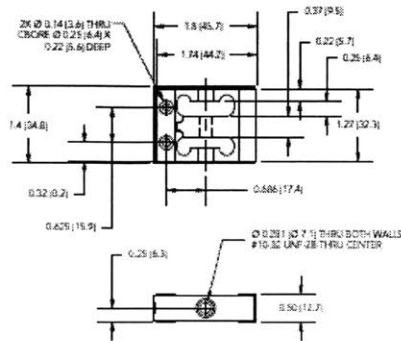




Model LSM300

2

DIMENSIONS inches [mm]



CAPACITIES

ITEM #	lb	N	Deflection (in.)	Natural Frequency (Hz)	Safe Overload (lb)
FSH03974	2.2	9.8	0.0080	280	250
FSH03975	5	22.2	0.0065	468	250
FSH03976	10	44.5	0.0060	687	250
FSH03977	25	111	0.0055	1134	250
FSH03978	50	222	0.0055	1593	250
FSH03979	100	445	0.0060	2157	250
FSH03980	200	890	0.0055	1773	400*

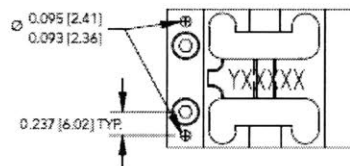
*If additional pins are used

WIRING CODE (WC2)

GREEN	+ EXCITATION
BLACK	- EXCITATION
WHITE	+ SIGNAL
RED	- SIGNAL

*Color code for this sensor is not FUTEK standard

ADDITIONAL HOLE LOCATIONS (200 LB ONLY)



Drawing Number: F11400

FUTEK reserves the right to modify its design and specifications without notice. Please visit www.futek.com/calculators for complete terms and conditions.

10 Thomas, Irvine, CA 92618 USA
Tel: (949) 465-0900
Fax: (949) 465-0905

www.futek.com



ROHS



A-2: Analog Devices Instrumentation Amplifier (selected pages) available online at <http://www.analog.com/en/products/amplifiers/instrumentation-amplifiers/ad8237.html#product-overview>



Micropower, Zero Drift, True Rail-to-Rail Instrumentation Amplifier

Data Sheet

AD8237

FEATURES

- Gain set with 2 external resistors
- Can achieve low gain drift at all gains
- Ideal for battery powered instruments
- Supply current: 115 μ A
- Rail-to-rail input and output
- Zero input crossover distortion
- Designed for excellent dc performance
 - Minimum CMRR: 106 dB
 - Maximum offset voltage drift: 0.3 μ V/ $^{\circ}$ C
 - Maximum gain error: 0.005% (all gains)
 - Maximum gain drift: 0.5 ppm/ $^{\circ}$ C (all gains)
 - Input bias current: 1 nA guaranteed to 125 $^{\circ}$ C
- Bandwidth mode pin (BW) to adjust compensation
- 8 kV HBM ESD rating
- RFI filter on-chip
- Single-supply operation: 1.8 V to 5.5 V
- 8-lead MSOP package

APPLICATIONS

- Bridge amplification
- Pressure measurement
- Medical instrumentation
- Thermocouple interface
- Portable systems
- Current measurement

GENERAL DESCRIPTION

The AD8237 is a micropower, zero drift, rail-to-rail input and output instrumentation amplifier. The relative match of two resistors sets any gain from 1 to 1000. The AD8237 has excellent gain accuracy performance that can be preserved at any gain with two ratio-matched resistors.

The AD8237 employs the indirect current feedback architecture to achieve a true rail-to-rail capability. Unlike conventional in-amps, the AD8237 can fully amplify signals with common-mode voltage at or even slightly beyond its supplies. This enables applications with high common-mode voltages to use smaller supplies and save power.

The AD8237 is an excellent choice for portable systems. With a minimum supply voltage of 1.8 V, a 115 μ A typical supply current, and wide input range, the AD8237 makes full use of a limited power budget, yet offers bandwidth and drift performance suitable for bench-top systems.

Rev. 0
Information furnished by Analog Devices is believed to be accurate and reliable. However, no responsibility is assumed by Analog Devices for its use, nor for any infringements of patents or other rights of third parties that may result from its use. Specifications subject to change without notice. No license is granted by implication or otherwise under any patent or patent rights of Analog Devices. Trademarks and registered trademarks are the property of their respective owners.

PIN CONFIGURATION

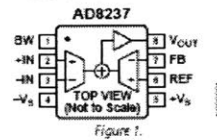


Figure 1.

Table 1. Instrumentation Amplifiers by Category¹

General Purpose	Zero Drift	Military Grade	Micropower	Digital Gain
AD8421	AD8237	AD620	AD8237	AD8250
AD8221/AD8222	AD8231	AD621	AD8420	AD8251
AD8220/AD8224	AD8293	AD524	AD8235/AD8236	AD8253
AD8228	AD8553	AD526	AD627	AD8231
AD8295	AD8556	AD524		
AD8226	AD8557			

¹ See www.analog.com for the latest Instrumentation amplifiers.

The AD8237 is available in an 8-lead MSOP package. Performance is specified over the full temperature range of -40 $^{\circ}$ C to +125 $^{\circ}$ C.

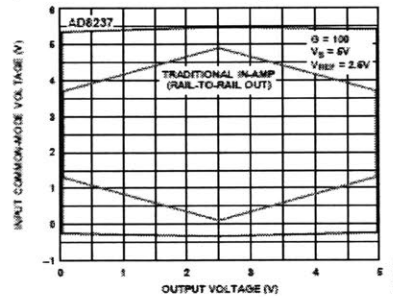


Figure 2. Input Common-Mode Voltage vs. Output Voltage, +Vs = 5 V, G = 100

One Technology Way, P.O. Box 9106, Norwood, MA 02062-9106, U.S.A.
Tel: 781.329.4700 www.analog.com
Fax: 781.461.3113 ©2012 Analog Devices, Inc. All rights reserved.

THEORY OF OPERATION

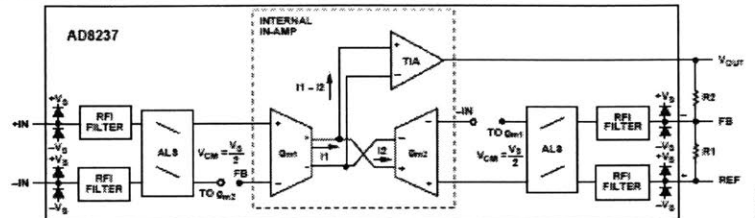


Figure 65. Simplified Schematic

ARCHITECTURE

The AD8237 is based on an indirect current feedback topology consisting of three amplifiers: two matched transconductance amplifiers that convert voltage to current, and one transimpedance amplifier, TIA, that converts current to voltage.

To understand how the AD8237 works, first consider only the internal in-amp. Assume a positive differential voltage is applied across the inputs of the transconductance amplifier, g_{m1} . This input voltage is converted into a differential current, I_1 , by the g_{m1} . Initially, I_2 is zero; therefore, I_1 is fed into the TIA, causing the output to increase. If there is feedback from the output of the TIA to the negative terminal of g_{m1} , and the positive terminal is held constant, the increasing output of the TIA causes I_2 , as shown, to increase. When it is assumed that the TIA has infinite gain, the loop is satisfied when I_2 equals I_1 . Because the gain of g_{m1} and g_{m2} are matched, this means that the differential input voltage across g_{m1} appears across the inputs of g_{m2} . This behavioral model is all that is needed for proper operation of the AD8237, and the rest of the circuit is for performance optimization.

The AD8237 employs a novel adaptive level shift (ALS) technique. This switched capacitor method shifts the common-mode level of the input signal to the optimal level for the in-amp while preserving the differential signal. Once this is accomplished, additional performance benefits can be achieved by using the internal in-amp to compare +IN to FB and -IN to REF. This is only practical because the signals emitting from the ALS blocks are all referred to the same common-mode potential.

In traditional instrumentation amplifiers, the input common-mode voltage can limit the available output swing, typically depicted in a hexagon plot of the input common-mode vs. the output voltage. Because of this limit, very few instrumentation amplifiers can measure small signals near either supply rail. Using the indirect current feedback topology and ALS, the AD8237 achieves a truly rail-to-rail characteristic. This increases power efficiency in many applications by allowing for power supply reduction.

The AD8237 includes an RFI filter to remove high frequency out-of-band signals without affecting input impedance and CMRR over frequency. Additionally, there is a bandwidth mode pin to adjust the compensation. For gains greater than or equal to 10, the bandwidth mode pin (BW) can be tied to +V₂ to change the compensation and increase the gain bandwidth product of the amplifier to 1 MHz. Otherwise, connect BW to -V₂ for a 200 kHz gain bandwidth product.

SETTING THE GAIN

There are several ways to configure the AD8237. The transfer function of the AD8237 in the configuration in Figure 65 is

$$V_{OUT} = G(V_{IN} - V_{REF}) + V_{REF}$$

where:

$$G = 1 + \frac{R2}{R1}$$

Table 7. Suggested Resistors for Various Gains (1% Resistors)

R1 (kΩ)	R2 (kΩ)	Gain
None	Short	1.00
49.9	49.9	2.00
20	80.6	5.03
10	90.9	10.09
5	95.3	20.06
2	97.6	49.8
1	100	101
1	200	201
1	499	500
1	1000	1001

Whereas the ratio of R2 to R1 sets the gain, the designer determines the absolute value of the resistors. Larger values reduce power consumption and output loading; smaller values limit the FB input bias current and input impedance errors. If the parallel combination of R1 and R2 is greater than about 30 kΩ, the resistors start to contribute to the noise. For best output swing and linearity, keep $(R1 + R2) \parallel R_i \geq 10 \text{ k}\Omega$.

Appendix B: Futek Load Cell Certificate of Conformance



FUTEK
ADVANCED SENSOR TECHNOLOGY, INC.

10 Thomas Drive, CA 92618 USA
Tel: (949) 445-0900
Fax: (949) 445-0902

CERTIFICATE OF CONFORMANCE

Certificate #: 1704130098

Model: LSM300	Item #: FSH03977	Capacity: 25 lb
Temperature: 73°F	Humidity: 47 %	Excitation: 10.00 (Vdc)
FS Load: 25 lb		

Tension

No.	S/N	Rin (Ω)	Rout (Ω)	FS Output (mV/V)	Zero Balance (mV/V)
1	715449	1.121	1.902	2.1551	-0.0043

This certifies that the listed sensor(s) and/or instrument(s) has been tested using equipment traceable to NIST and conforms to the manufacturing and/or final product specifications per printed material or purchase order. Supporting documentation relative to traceability is on file and is available for examination upon request.

Tested by: David Campos	4/13/2017
--------------------------------	-----------

Sensor Solution Source
Load - Torque - Pressure - Multi-Axis - Calibration - Instruments - Software
www.futek.com



